FIRST T_e PROFILE RESULTS FROM THE JET LIDAR-THOMSON SCATTERING SYSTEM

C Gowers, B Brown, A Gadd, M Gadeberg, K Hirsch+, H Murmann*
P Nielsen, H Salzmann+, C Schrödter°
JET Joint Undertaking, Abingdon, Oxon OX14 3EA, UK
+ On attachment from Institut für Plasmaforschung, Universität Stuttgart, 7000 Stuttgart 80, FRG
* Max-Planck-Institut für Plasmaphysik, 8046 Garching, FRG
° Max-Planck-Institut für Quantenoptik, 8046 Garching, FRG

INTRODUCTION - The application of 180° Thomson scattering using short (~ 300 ps) laser pulses for measuring electron temperature and density profiles in large fusion devices was proposed in /1/. With the short laser pulse method, spatial resolution along the laser beam is achieved by high-speed detection techniques allowing time-of-flight measurements /2/. This LIDAR (Light Detection and Ranging) technique was applied for the first time on the JET tokamak. The JET LIDAR Thomson Scattering diagnostic is described in outline below. The first electron temperature profiles obtained with the system are presented and compared with those obtained using other JET diagnostics.

THE LIDAR THOMSON SCATTERING SYSTEM - Figure 1 shows the optical set-up of the diagnostic. A ruby laser pulse of 220 ps duration is directed radially into the tokamak vessel in the equatorial plane and dumped on a carbon tile at the inner torus wall. The laser beam inside the vessel has a constant diameter of 50 mm. During the measurements described here, the laser (JK LASERS (Lumonics) Rugby, UK), capable of 5 J operation at up to 0.5 Hz repetition rate, was operated at 2 J and single shot.

a) Laser - The laser consists of an actively mode-locked oscillator, two single pulse selectors (Pockels cell shutters) in series to attenuate spurious background pulses and four stages of amplification. Two vacuum spatial filters are also included in the amplifier train.
b) Input Optics - In the initial set up described here the laser beam was directed to the Torus 60 m away by a simple mirror system. Imaging optics and a vacuum pinhole system will be used in the future.
c) Collection Optics - The backscattered light is collected by a folded spherical mirror system through an array of six windows surrounding the central laser input window on the JET vessel. Its effective solid angle of collection is 5.5×10^{-3} sr. The collection optics and the labyrinth mirror system, which transmits the collected light through the 2.2 m thick biological shield, is shared with the single spatial point 90° Thomson scattering system on JET /3/, for which it was constructed. The two collected light beams are separated from each other in the entrance slit plane of the polychromator of the single point scattering system. The entrance slit is surrounded by a broadband mirror which directs approximately 95% of the scattered light from the LIDAR laser beam into the LIDAR polychromator.
d) Polychromator - The three main features of the LIDAR polychromator are extremely high optical throughput of 1 cm^2sr, high average

transmission of the six spectral channels (about 70%) and rejection of ruby laser stray light by a factor greater than 10^5. This performance is achieved with a filter polychromator in which the incident light is shone onto a stack of short wave pass interference edge filters with decreasing cut-on wavelengths, the filters being tilted slightly with respect to each other /4/. The transmission bandwidth of a spectral channel observing reflected light from this filter stack is defined by the cut-on wavelengths of two adjacent filters of the stack and by a suitably chosen coloured glass filter in front of each detector. Additional short wave pass filters in front of each detector improve further the rejection of stray ruby laser light. The collection mirrors, which are illuminated homogenously by scattered light during the passage of the laser pulse through the plasma, are imaged onto the filter stack. In this way slight variations of the cut-on wavelengths across the surface of the 200 mm diameter edge filters are averaged in the same way when the scattering volume moves through the plasma. In the course of the first measurements, reported here, only four of the available six spectral channels were used. Their transmission bands were 660-626 nm, 639-601 nm, 598-534 nm and 530-480 nm, respectively.

e) Detectors and Digitizers - The high speed detection of the backscattered light pulse is accomplished using proximity focused MCP photomultipliers (ITT F 4128) with 20 mm diameter photocathodes. The output signals are registered by TEK 7912 AD transient digitizers with 7 A 29 vertical amplifier plugs-in. The overall bandwidth of the complete detection and registration system is approximately 700 MHz.

f) Stray Light Suppression - Ruby laser stray light pulses arriving at the detectors before the scattered signal are suppressed very effectively (by a factor of 10^{13} /4/) by gating the photocathode to MCP gap of the detectors. The flat top of the gate is about 30 ns long and the ringing, coupled to the detector output by the 10 ns risetime/150 V amplitude gating pulse, is kept below 10 mV. An intense stray light pulse occurs after the measurement when the laser pulse strikes the carbon tile dump at the Torus inner wall. This stray light burst causes a 300 V/0.5 ns electrical pulse at the output of the detectors and a high speed, pulse clipping diode circuit in the signal lead is used to protect the vertical amplifier plug-ins of the digitizers /5/.

RESULTS - Figure 2 shows an overlay of the detector signals recorded by the digitizers both when the laser was pulsed a) during a JET pulse (full curve) and b) with no plasma present in the JET vacuum vessel (dashed curve).

The base lines prior to gating on the detector appear in region 1. For region 2, as the detectors were gated on, a 'switch on' peak was observed due mostly to the presence of some spurious laser stimulated fluorescence from a (temporary) mask surrouding the laser input mirror figure 1. This spurious source of stray light will be avoided in the future when the imaging input optics is installed. The difference between the continuous and dashed curves in region 3 shows the expected low plasma light level, a merit of the LIDAR system resulting from the short integration time in the detection system. Thus, the difference between the two curves in region 4 is predominantly due to the scattered light from the laser pulse as it propagates through the plasma.

The signal traces are effectively terminated by the arrival of the stray light burst caused by the laser pulse striking the carbon dump tile at t ≃ 48 ns. No stray light pulses from the main laser pulse were observed during the 17 ns scattering record, region 4, but the effect of a low level (10^{-3}) laser pre-pulse striking the dump ~ 2 ns before the main pulse can be seen on digitizer 1 at ~ 46 ns. The pre-pulse has since been removed by more careful setting up of the laser oscillator.
The scattered light signals from figure 2 have been time correlated using the data obtained from a test experiment in which the peak of the stray termination pulse was displayed by using optical attenuation in front of each detector. The time marker so obtained is also indicated in figure 2. In this first analysis, the electron temperature has been fitted to each 500 ps time averaged segment of the channel data in region 4. The resultant T_e profile is shown in figure 3a where it is compared with the partial T_e profile obtained from the JET ECE diagnostic /6/. At this time during the discharge ~ 6 MW of RF heating power were being applied to the plasma, producing a moderately high central electron temperature.
In contrast figure 3b shows a low T_e case just after pellet injection in which a central electron temperature of a factor of 4 lower is indicated. Once again good agreement between the profile data from the two diagnostics is obtained. In fact the LIDAR system to date has been used successfully over the 0.2-5.0 keV temperature range. Also from figure 3b, the steep temperature gradient around 2.6 to 2.8 m indicates that the spatial resolution of the diagnostic is 0.10-0.15 m as expected.

CONCLUSION - The first electron temperature profiles have been obtained with the LIDAR Thomson Scattering diagnostic on the JET Tokamak.
The full T_e profiles are in good agreement over a wide range of plasma conditions with partial profiles obtained by the ECE technique.
A spatial resolution for the diagnostic of 0.10-0.15 m is indicated with this preliminary data set.

ACKNOWLEDGEMENT - It is a pleasure for the authors to acknowledge the support and encouragement received from all their colleagues at JET, Risø National Laboratory, Denmark, Stuttgart University and MPQ Garching FRG. We are also indebted to the JET ECE group for the use of their temperature profile data.

REFERENCES

/1/ H Salzmann, K Hirsch, Rev Sci Instr 55 (84), 457.
/2/ R Kristal, Diag. for Fusion Exps, Varenna 1978, p 617, EUR 6123.
/3/ P Nielsen, Course on Diagnostic for Fusion Reactor Conditions, Varenna 1982, Vol 1, p 225, EUR 8351-1EN.
/4/ C Gowers, M Gadeberg, K Hirsch, P Nielsen, H Salzmann et al, Course and Workshop on Basic and Advanced Fusion Plasma Diagnostic Techniques, Varenna 1986, page 205, Vol 2.
/5/ J Bundgaard et al, private communication, Risø National Laboratory.
/6/ A E Costley et al, in Controlled Fusion and Plasma Physics (Proc 12th European Conference, Budapest 1985) 9F-I (1985) 227.

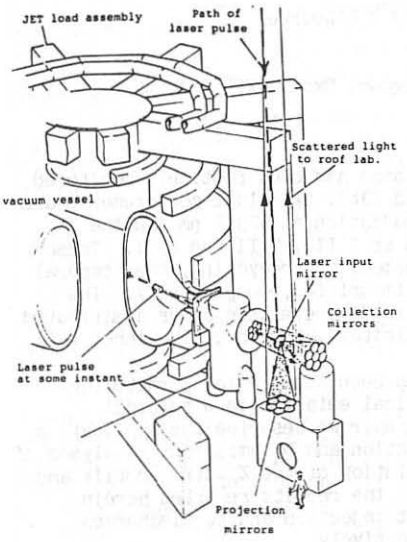

FIG 1. SCHEMATIC OF LIDAR THOMSON SCATTERING DIAGNOSTIC ON JET

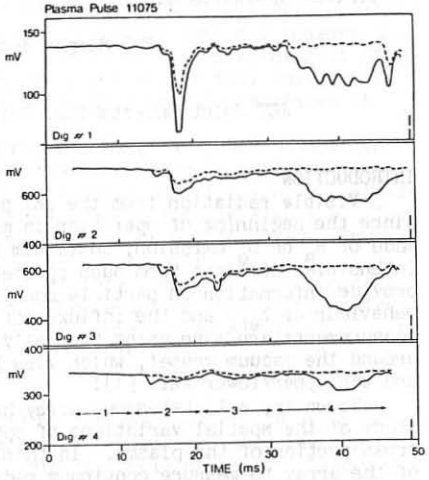

Signals output by the digitisers (a) During a Plasma pulse (full curve)
(b) During 'Laser only' shot - no plasma (dashed)
Region 1 - Detector output prior to gating on (baseline)
Region 2 - Detector output during gating on
Region 3 - Detector output due to Plasma light
Region 4 - Detector output during period laser pulse traverses plasma

The vertical bar indicates the fiducial marker for each digitiser signal

Fig 2

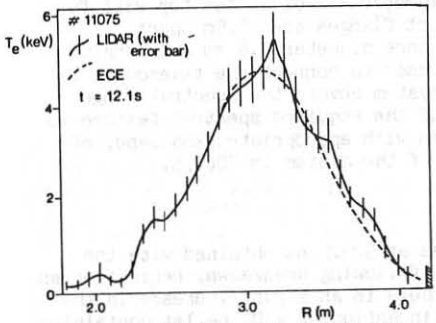

LIDAR and ECE T_e profiles during RF Heating

Fig 3a

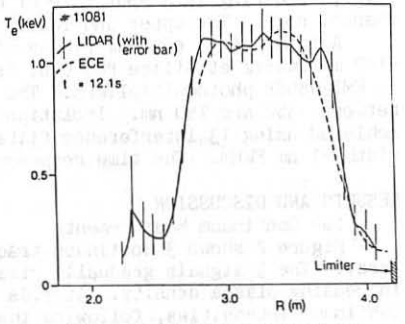

LIDAR and ECE T_e profiles during Pellet Injection

Fig 3b